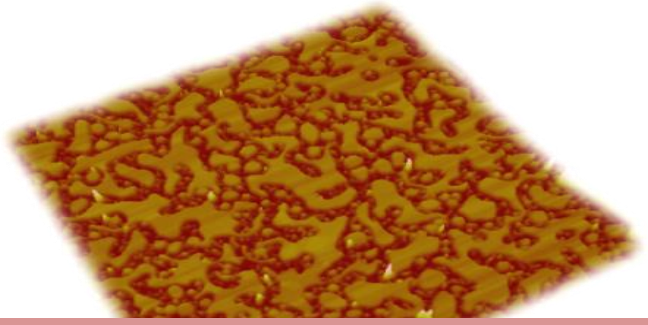

FORMATION AND CHARACTERIZATION OF MODEL CELL MEMBRANES AND THEIR INTERACTION WITH MAGNETIC NANOPARTICLES

Silvia Ruiz Rincón

Supervisors:

Dr. Pilar Cea Mingueza

Physical Chemistry Department and Institute of Nanoscience of Aragón. University of Zaragoza

Dr. Jesús Martínez de la Fuente

Institute of Materials Science of Aragón. CSIC / University of Zaragoza

PILAR CEA MINGUEZA, profesora titular del Departamento de Química Física de la Universidad de Zaragoza y JESUS MARTÍNEZ DE LA FUENTE, científico titular del Instituto de Ciencia de los Materiales de Aragón (ICMA) perteneciente al Consejo Superior de Investigaciones Científicas

CERTIFICAN:

Que el trabajo presentado en esta memoria por Silvia Ruiz Rincón como Proyecto Final del Máster Universitario en Materiales Nanoestructurados para Aplicaciones Nanotecnológicas y que lleva como título *"Formation and Characterization of model cell membranes and their interaction with magnetic nanoparticles"* , ha sido desarrollado bajo su dirección, autorizando la presentación del mismo para su calificación por el Tribunal correspondiente.

Y para que así conste, se expide el presente certificado en Zaragoza, a 30 de noviembre de 2015.

Table of content

Acknowledgements

Firstly, I would like to express my sincere gratitude to my supervisors Pilar Cea and Jesús Martínez de La Fuente for providing me an opportunity to join their labteam where I have enjoyed working and learning every day.

To Dr. Pilar Cea for her patience, motivation and immense knowledge, for giving advice to improve, her guidance really helped me, and for everything I have learned, not only related to scientific skills but also to my personal growth. THANKS.

To Dr. Jesús Martínez de La Fuente for being very thoughtful and attentive to everything I needed, helping me with his good advice and making easier my work. THANKS.

I thank all the staff of the LMA and Raluca for assisting me during my research to achieve my goals.

I thank my fellow labmates for sharing hour and hour to work, thanks to support me, help me and make me easier this year of work.

I would like to thank Alex for her invaluably constructive criticism and friendly advice during my project work. I am sincerely grateful to him for sharing his truthful and clarifying views on a number of issues related to the project, for sharing with me all his knowledge about AFM and other skills. Without his help my work would not have been the same. MANY THANKS. In addition to all my acquired knowledge, I have gained a friend.

Last but not least, I would like to thank my family: my parents and my sister for supporting me, giving good advice and assisting me to improve. Without their effort and dedication I would not have been able to achieve my purposes. My sincere thank. Alberto, thanks for being incredibly understanding, supportive, and most of all, patient and make me a better person.

Finally, I would also like to acknowledge INA for the research summer grant in the group PLATON and NAP

Abstract

Understanding the process occurred in cell membranes as well as their interaction with external agents such as Magnetic Nanoparticles (MNPs) is a goal of main importance in biomedicine. In this work model cell membranes of a mixture of 1, 2-dipalmitoyl-sn-glycero-3-phosphocholine (DPPC) and cholesterol were transferred onto mica substrates by Langmuir-Blodgett technique (LB) to mimic a real cell membrane. The high quality and chemical structure of the monolayers formed were confirmed by means of Atomic Force Microscopy (AFM) imaging and Contact Angle measurements. Due to the amphiphilic features of the compounds used in this work, a study of the stability of the monolayer in liquid media was carried out observing as the monolayer re-assembled into bilayer. This behaviour was explained by means of Force Spectroscopy (FS) studies with a noticeable increase in the breakthrough force values. Furthermore, the deposition of MNPs onto monolayer was carried out by LB in a successful way obtaining a well-covered distribution of MNPs with the final purpose of study the membrane response when it is exposed to alternating magnetic fields.

Chapter 1. Objectives

1.1 General training objectives

The general objectives of a final project corresponding to the Master´s Degree in *Nanostructured Materials for Nanotechnology Applications* from the University of Zaragoza are the acquisition and development of diverse skills in the nanoscience and nanotechnology fields. In particular, the competences that a master candidate should have achieved by his/her graduation, and I believe I have achieved, include the following:

- Knowledge and understanding in the area of Nanotechnology.
- Deep understanding of the different methodologies applied in Nanotechnology.
- Ability to critically and systematically integrate the acquired knowledge and analyze, evaluate and handle complex occurrences, issues and situations.
- Awareness of the possibilities and limitations of methods, techniques and their applications in different research areas.
- Skills which are required for participation in research and development work or in other independent work of a qualified nature.
- Identify and formulate issues, use of adequate methods, qualified tasks and thereby contribute to the evolution of knowledge.
- Being conscious about the difficulties arisen during the realization of the project and being able to sort out those scientific problems in a proper way.
- Incorporation of scientific habits as an essential condition to take effective profit of the learning process as a mean of personal development.
- Ability to present and discuss conclusions and the knowledge and the arguments on which these conclusions are based.
- Oral and written skills in the English language, using the vocabulary and specific terminology in the scientific context, and showing initiative and self-confidence in the course of the oral presentation.
- Consolidation of personal and social capabilities to behave in a responsible and autonomous way by developing a critical sense.

2.2 Scientific objectives of the final master project entitled "Formation and Characterization of Model Cell Membranes and their Interaction with Magnetic Nanoparticles"

The specific objectives that my final master project supervisors defined by the beginning of this work were:

- Fabrication of mono and/or bilayer mixed films incorporating phospholipids and cholesterol by the Langmuir-Blodgett (LB) method to mimic the cell membrane.
- Characterization of these LB films to determine their morphology and stability.
- Immobilization of magnetic nanoparticles onto the mixed phospholipic and cholesterol films.
- Analyze and understand effects induced by the application of an alternating magnetic field (hyperthermia) on the mixed films decorated with the magnetic nanoparticles.

Chapter 2. Introduction

Over the last few years there has been a significant interest focused on nanomaterials owing to a wide variety of applications in different fields of study ranging from physics, engineering or science of materials, to medicine, biology or chemistry.

Biological membranes are extremely complex and make research work very difficult. As a consequence, a great effort is required to properly understand all the process that take place. For this reason, artificial model membranes have been developed during the recent years and play an important role in clearing up the physical and chemical features of membranes and how these contribute to membrane functions. All these process would be probably difficult or even impossible to be studied otherwise.[1,2,3] In this context, the popularity of the deposition of model cell membranes has grown because of its wide biotechnological applications ranging from sensor design[4] to the study of membrane cell interactions.[5] This has been supported by the emergence of a multitude of surface characterization techniques.[6]

How is possible to mimic a cell membrane? For the recent years, phospholipid layer deposited onto solid surface have been the most commonly used experimental cell surface model. There are several experimental techniques which allow building model cell membranes such as lipid vesicles, monolayers at air-water interface and different types of supported lipid bilayers (SBL).[7,8] These techniques have been developed and improved since in 1960s Mueller et al. developed the first system for the investigation of the electrical properties of a planar phospholipid bilayer.[9] In particular, the technique chosen in this work for mimicking a cell membrane was Langmuir-Blodgett whose applications in this field are reported elsewhere.[10,3,11] The transfer of phospholipid monolayer onto hydrophilic substrate by LB had been attempted before by Levin et al. in 1968[12] although they had not found application in biophysical research. In contrast, in 1972 Kühn et al[13] collected numerous studies on fatty acid as well as in 1977 Korenbrot and co-workers[14] used phospholipids LB films for device fabrication. The advantages of using LB technique are the possibility to control the parameters needed to reproduce biological conditions as well as the achievement of ordered films with well-defined molecular orientation and reproducible results.

In the area of Biomedicine, one of the most interesting nanomaterials from the point of view of their physical features are the magnetic nanoparticles (MNPs) [15,16] due to the facility of MNPs to be heated after applying an outer alternating magnetic field, turning them promisingly suitable to be used in hyperthermia studies.[17,18,19] In this regard, it should be noted that hyperthermia is a type of treatment applied as an adjunctive therapy with other established cancer treatments such as radiotherapy and chemotherapy. By means of increasing the local temperature when an external alternating magnetic field is applied, unhealthy cells can be eventually damaged. One of the most interesting cellular compartment to obtain more effectiveness is over the membrane of the cell because of the fact that many important biological processes occur there.

Accordingly, the aim of this project is to mimic a cell membrane and analyze the interactions occurred between the membrane and the magnetic nanoparticles. To know how this interaction takes place and its efficacy constitutes an important step in future research.

As preliminary studies have to be carried out to optimize and to have a clear understanding about the system, this work is focused on the effects occurred in phospholipid monolayers due to there are significant advantages to determine the effects of the interaction between the nanoparticles and the hydrophobic part of the layer as well as the possibility to have a high control of phospholipid packing, which can mimic various stages of the cell membrane structuring. In this regard, phospholipid monolayer has also been employed successfully to characterize specific interactions between proteins and lipid membranes.[20]

In order to achieve a model cell membrane a mixture of 1, 2-dipalmitoyl-sn-glycero-3-phosphocholine (DPPC) and cholesterol was deposited onto a solid substrate. It can be observed the structure of these compounds in Figure 1.

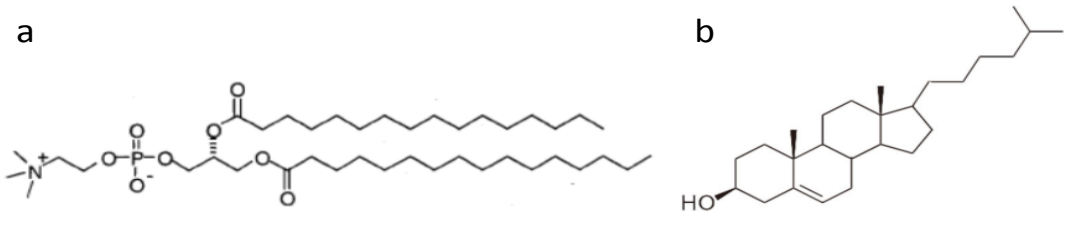

Figure. 1 (a) Structure of DPPC; (b) Structure of Cholesterol.

The solid substrate chosen in this work was mica, the election of the substrate is very important in the results, due to the substrate has to be capable of support high quality membranes. Consequently, it should be hydrophilic, smooth and clean.[21, 22]

Another advantage to work with monolayers is due to the amphiphilic nature of the compounds shown in Figure 1, consisting of a hydrophilic part (attached to substrate due to their affinity) and a hydrophobic part exposed at the interface, phospholipid membranes are capable of organizing themselves as well as associated with nanoparticles or other species within the membrane or at its surface.

The cholesterol, the other compound shown in figure 1, is well-known that is an important lipid of mammalian cells and modulate the fluidity of cell membranes[23] as well as the cholesterol increases the structural order of the phospholipid chains.[24]

How is possible to study the interaction between the nanoparticles and the cell membrane? The magnetite nanoparticles were also deposited by LB onto the mixed monolayer previously formed. The capping of the nanoparticles is another issue to take into account due to the fact that this capping will be the specific part which will be attached to the lipid monolayer. In this context, Atomic Force Microscopy (AFM) is a powerful tool in bio-membrane research to study the effect of the NPs on the model cell membranes.[25,26,27] It enables to study the morphological structure, physical properties as adhesion and bimolecular interaction, as well as, to study mechanical properties of the mimic membranes in a quantitative way by force spectroscopy.

All of these results are collected in this final master project, starting with the formation of a model cell membrane and the study of different tests to confirm the properties and the quality of the monolayer formed. Secondly, a study of the stability of the monolayer in liquid media considering the amphiphilic nature of the compounds used is carried out. Thirdly, the deposition of the magnetic nanoparticles onto the monolayer is optimized to achieve a good surface distribution and coverage. Finally, this work finishes with some preliminary hyperthermia studies which are the beginning to future works based on the precursory results obtained.

Chapter 3. Experimental section

3.1 Materials and substrates

Table I gathers the reactants used in this work together with their CAS number, purity as well as the supplier of these products.

Table I. Reactants, CAS number, and supplier.

Compound	CAS number	Purity	Purchased from
DPPC	63-89-8	99.9 %	Sigma-Aldrich
Cholesterol	57-88-5	99.9 %	Sigma-Aldrich
Water		Milli-Pore Milli-Q (resistivity 18.2 MΩ·cm)	Obtained from a Millipore water purification system at INA
Chloroform	67-66-3	99 % (ethanol 1 %)	Sigma-Aldrich
Ethanol	64-17-5	99.5 %	Panreac
Acetone	200-662-2	99.5 %	Panreac

LB films were deposited onto mica substrates provided by Electron Microscopy Sciences Company (Cat. #71851-05, sheet size 1" x 3"; 25 x 75 mm and thickness 0.26 -0.31 mm). . These mica substrates were cut by using a pair of scissors into ca. 1 x 1 cm^2 pieces and cleavage with a cello tape prior to their use.

Magnetic Fe_3O_4 nanoparticles with a mean diameter of 8 nm were used in this work. These nanoparticles were covered with oleic acid and oleylamine. The synthesis and functionalization of these nanoparticles was done at the group of Jesús Martínez de la Fuente.

3.2 Experimental techniques

3.2.1 The Langmuir- Blodgett technique

Langmuir and Langmuir Blodgett films were prepared using a NIMA-KSV commercial trough housed in a constant temperature (20±1 ºC) clean room. Figure 2 shows a photograph of the LB trough used in this work. The trough is made of the following parts:[28]

- A Teflon cuvette where the liquid suphase is situated.
- Two barriers which allow the compression and the formation of the monolayer.
- A Wilhelmy paper plate pressure sensor used to measure the surface pressure (π) upon the compression of the film.
- A dipper to hold the substrate onto which the LB films are transferred.

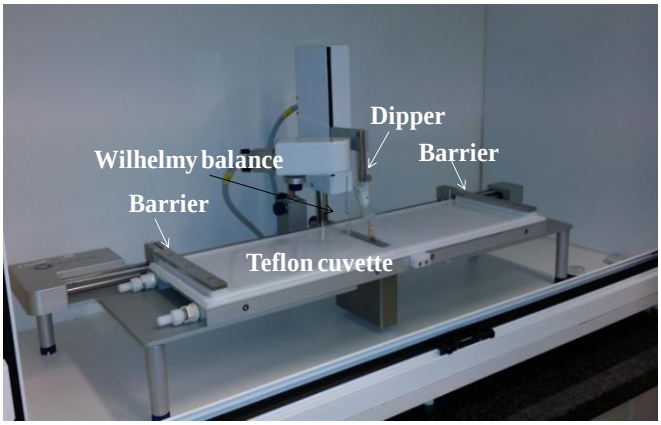

Figure 2. Photograph of the NIMA- KSV trough used in this work.

To construct the Langmuir films 750 μL of a 10^{-4} M mixed solution of the DPPC and cholesterol in chloroform (DPPC mole fractions of 1, 0.75, 0.5, 0.25 and 0) was spread by a syringe held very close to the surface (Figure 3), allowing the surface pressure to return to a value close to zero between each addition. After waiting about fifteen minutes to allow the solvent to evaporate, slow compression of the film began at a speed of 6 $nm^2 \cdot molecule^{-1} \cdot min^{-1}$. Each isotherm was recorded three times to ensure the reproducibility of the obtained data. The monolayers at the air-water interface were transferred onto solid supports at a constant surface pressure of 35 $mN \cdot m^{-1}$ by the vertical dipping method (dipping speed was 1 $mm \cdot min^{-1}$) onto cleavage mica substrates.

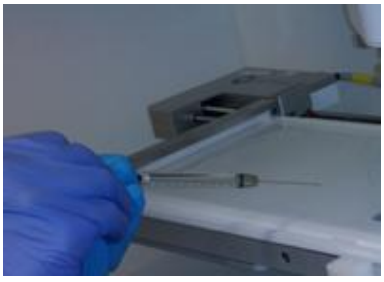

Figure 3. Photograph taken during the spreading process by means of a Hamilton syringe.

Additional information about the technique is included in Annex section.

3.2.2 Atomic Force Microscopy (AFM)

Atomic Force Microscopy experiments were performed by means of a Multimode 8 microscope equipped with a Nanoscope V control unit from Bruker at a scan rate of 1.0–1.2 Hz, using Tapping and Peak-Force modes. This microscope belongs to the Advanced Microscopy Laboratory (LMA) at the University of Zaragoza. The data were collected using RFESP (75–100 kHz, and 1–5 N m^{-1}, from Bruker) and ScanAsyst-Air-HR (130-160 kHz, and 0.4-0.6 N m^{-1}, from Bruker) tips for the images recorded in air. In the case of liquid measurements, SNL-C (40-75 kHz, and 0.24 N m^{-1}, from Bruker) and ScanAsyst-Liquid (100-200 kHz, and 0.7 N m^{-1}, from Bruker) tips were used. Images were typically recorded with scan rates of 1 $Hz \cdot line^{-1}$, 512 lines and force ranging 0.2-2 nN. Differences in height between monolayer domains were determined by performing section analysis.

Additional information about the technique is included in Annex section.

3.2.3 Contact Angle measurements

Contact angle experiments were performed with a commercial optical tensiometer Theta Lite TL 101 from Attension (Figure 4).

Figure 4. Theta Lite Optical Tensiometer used in this work.

In order to measure the contact angle of a liquid onto a solid surface, the sample is placed on a plane platform, just below a needle from which a drop of liquid is deposited onto the sample. Thereafter, the computer software collects readings of the contact angle at different times. With this system, the data set will have statistical meaning. The process is repeated at least three times in distinct places of each sample to test the reproducibility of the data.

3.2.4 Hyperthermia measurements

Hyperthermia experiments were performed with DM100 Series equipment by nB nanoScale Biomagnetics Company (Figure 5).

In order to measure, the sample is placed in a test tube, previously cut in the right dimensions to adjust to the required area. Measurements were carried out at 836 KHz for 90 minutes with an applied alternating magnetic field of 252 Gauss to properly detect the changes occurred.

Figure 5. Hyperthermia equipment used in this work

Chapter 4. Results and discussion

4.1 Surface pressure - area per molecule isotherms: pure and mixed compounds

Figure 6 shows the surface pressure vs. area per molecule isotherms (π-*A*) of pure DPPC and cholesterol as well as their mixtures of different mole fractions. In all cases the initial area per molecule was 1.4 $nm^2 \cdot molecule^{-1}$. Pure DPPC and pure cholesterol π-*A* isotherms as well as their mixtures have been reported before and the ones presented in this work are in good agreement with the literature.[29,30] .The π-*A* isotherm of DPPC is clearly characterized by a first gas phase in the 1.40- 1.05 nm^2 region followed by the liquid expanded phase (LE) in the 1.05-0.80 nm^2. Afterwards, the monolayer enters in the phase transition from the liquid expanded (LE) to the liquid condensed (LC) state (0.80-0.60 nm^2). Finally, the solid (S) phase starts at 0.47 nm^2 and the collapse of the monolayer is observed at ca. 57 $mN \cdot m^{-1}$. The π-*A* isotherm of

cholesterol is characterized by a lift-off in the isotherm at 0.45 nm^2 after which there is a monotonous increase in the surface pressure upon compression. The collapse of the cholesterol monolayer takes place at ca. 44 $mN \cdot m^{-1}$. The mixed monolayers result in surface pressure vs. area per molecule isotherms with intermediate behaviors as can be observed in Figure 6.

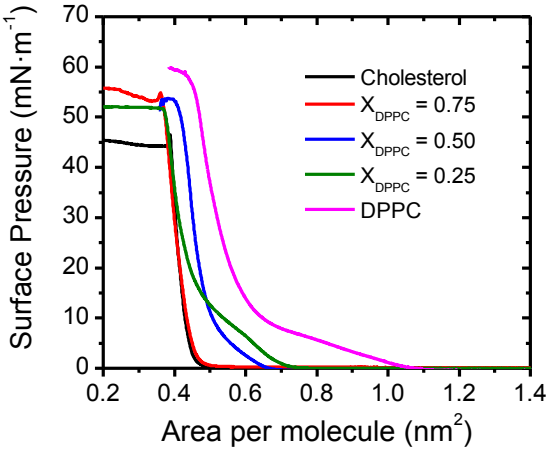

Figure 6. Surface pressure- area per molecule (π-A) isotherms for DPPC, cholesterol and mixed monolayers for 0.25, 0.5 and 0.75 DPPC mole fractions.

To obtain information about the condensing effect of the cholesterol on the DPPC monolayers, a study of the excess area per molecule in the mixed monolayer was made. In this context, if *A* corresponds to the area per molecule and π correlates to the surface pressure, then the excess area can be calculated by using the following equation:[30]

$$A^{EXC} = A_{12} - A_{12}^{id} = A_{12} - (A_1x_1 + A_2x_2) \qquad (1)$$

where A_1 and A_2 are mean molecular areas of the pure compounds DPPC and cholesterol, respectively, at a specific surface pressure; x_1 and x_2 are the mole fractions of compounds in the mixture solution, and A_{12} is the area per molecule in the mixed film. For completely immiscible or ideal mixed monolayers, the excess area is zero. In contrast, positive or negative excess areas are indicative of molecular interactions between the two compounds. Thus, positive deviations of the excess area in a mixed

system imply some type of repulsive interactions. On the contrary, negative deviations mean increased attractive interactions between the compounds.[31]

Figure 7 shows the excess area per molecule at 20, 30, 35 and 40 $mN \cdot m^{-1}$. The excess area per molecule is negative for the whole range of mole fraction which is indicative of strong attractive interactions between DPPC and cholesterol in the mixed films. The presence of two minima in the excess area vs. mole fraction plot has been interpreted before in terms of phase separation, with one of phases enriched with DPPC and the other one with cholesterol.[31]

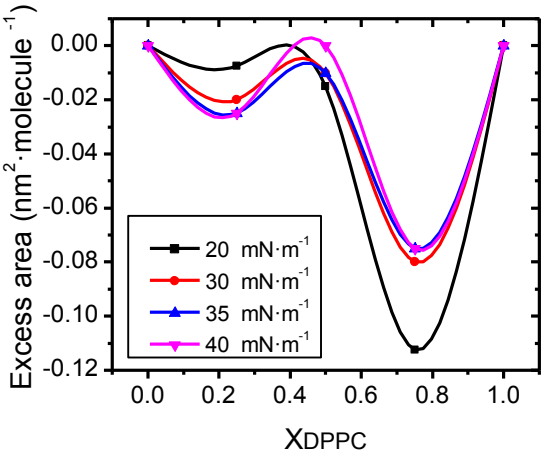

Figure 7. Excess area versus DPPC mole fraction for mixed DPPC/cholesterol monolayers

4.2 Optimization of the surface pressure of transference

The substrate chosen in this work to transfer the LB films was mica. Mica is a hydrophilic material and it provides a very flat surface that permits the study of the morphology of the covering layers with the AFM without inducing a sublayer roughness structure that could make difficult the interpretations of the AFM images. Mica substrates were initially immersed in the water subphase and withdrawn after the target surface pressure of transference was reached. Therefore, the hydrophilic groups in the monolayer are in contact with the mica surface (Figure 8).

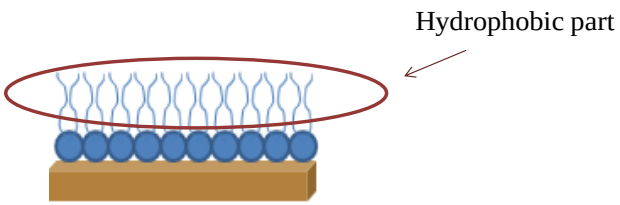

Figure 8. Cartoon showing the architecture of a monolayer of DPPC deposited onto a mica substrate.

In order to optimize the surface pressure of transference DPPC monolayers were transferred at a surface pressure of 25 and 35 $mN \cdot m^{-1}$ and the AFM images of these films are shown in Figure 9. The monolayers transferred at 25 $mN \cdot m^{-1}$clearly show the presence of holes, i.e. regions of mica not well covered by the monolayer. In contrast, AFM images for films transferred at 35 $mN \cdot m^{-1}$ evidence the formation of highly homogeneous and compact films free of holes or three dimensional defects. This result is in agreement with previous literature on these types of films.[29,30, 32] Therefore, all the LB films described henceforward have been transferred at this surface pressure of transference.

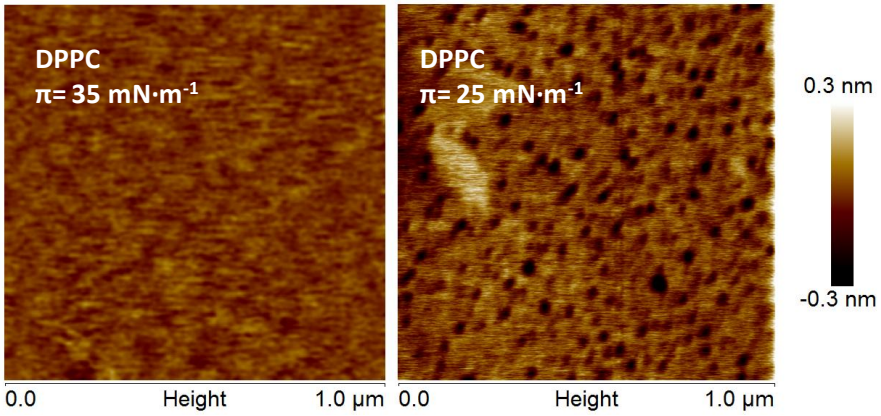

Figure 9. 1.0 x 1.0 μm^2 AFM topographic images for DPPC monolayers transferred at: (a) 35 $mN \cdot m^{-1}$ (b) 25 $mN \cdot m^{-1}$

4.3 Study of the ratio of transference

The ratio of transference provides information about the amount of material that can be transferred from a Langmuir film onto a solid substrate. The ratio of transference at a certain surface pressure can be determined using the following equation: [10]

$$\alpha = \frac{Sf}{S0} \qquad (2)$$

where S_f is the reduction of the monolayer area at the air-liquid interface and S_0 is the geometrical area of the substrate. The value of α is in the 0 to 1 range. The closer to 1 is the value of α, the better the process of transference is. In this work this value was determined directly upon the transference process with the aid of the software of the NIMA-KSV trough. The ratio of transference for a single layer of DPPC, cholesterol and their mixtures onto mica substrates was 1.

4.4 Morphological study of DPPC, cholesterol and the mixed films of DPPC/cholesterol by AFM

In order to assess the quality of the monolayers formed by LB, a systematic study of their topographical features by AFM was carried out. The results obtained can be observed in this section. Thus, figure 10 shows the AFM images for the pure DPPC and cholesterol monolayers on mica as well as the images of mixed monolayers of these compounds at the molar fractions studied in this work.

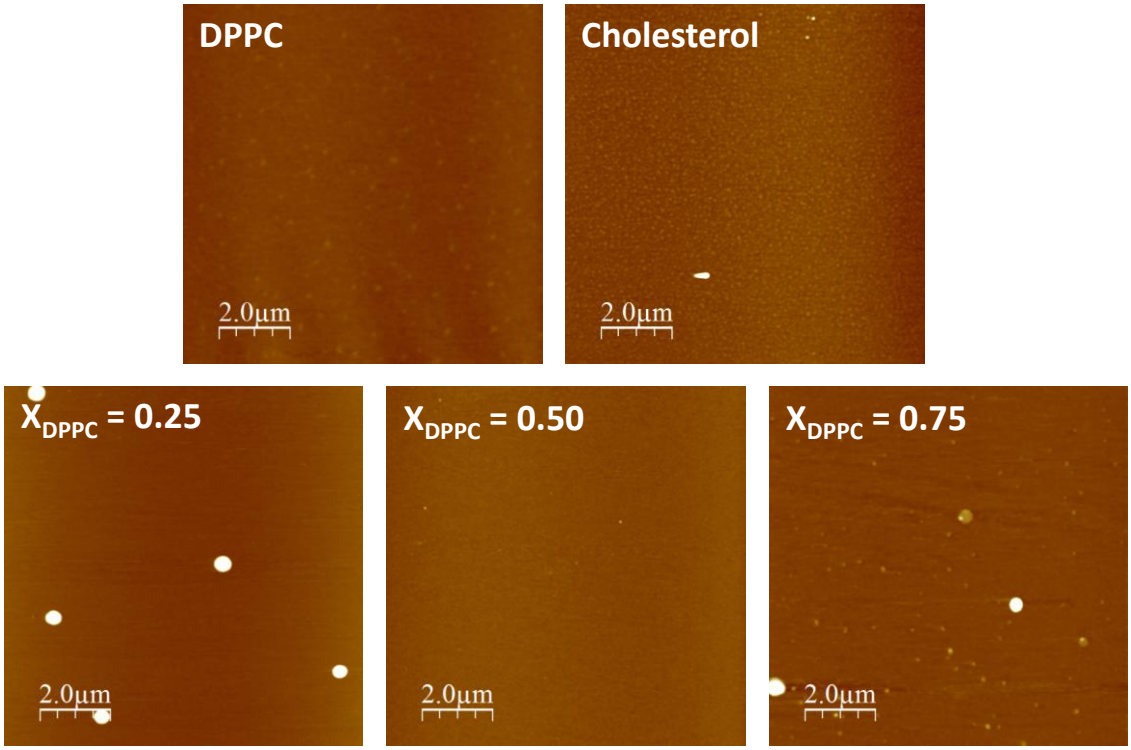

Figure 10. 10 x 10 µm^2 AFM topographic images for DPPC and cholesterol monolayers transferred onto mica substrates as well as the mixed films at the indicated mole fractions.

AFM images reveal that both pure DPPC and cholesterol monolayers are very homogeneous. In contrast, mixed monolayers exhibit a distinct behavior. The monolayer with a mole fraction of 0.5 is unambiguously the most homogeneous and remains free of three dimensional defects. Moreover, no domains are distinguished. In contrast, layers with x_{DPPC} = 0.25 and x_{DPPC} = 0.75 show the presence of three dimensional rounded spots with a height in the 4-6 nm range that result in less homogenous films.[33] [34] Table II shows the Root mean Square (RMS) roughness values for the studied monolayers.

Table II. RMS roughness values for the indicated monolayers

Monolayer	RMS roughness (nm)
DPPC	0.18
x_{DPPC} = 0.25	0.64
x_{DPPC} = 0.5	0.11
x_{DPPC} = 0.75	1.28
Cholesterol	0.09

From the AFM images and the roughness values it can be concluded that a mole fraction of 0.5 is an optimum one to obtain homogeneous mixed films free of defects. Consequently, we have used this mole fraction for the subsequent studies in this work.

The thickness of the x_{DPPC} = 0.5 monolayer was determined by scratching the film with the AFM tip, obtaining a value of ca. 2.2 nm, Figure 11, which is in very good agreement with the formation of a monomolecular layer as reported elsewhere.[35] This scratching technique has been shown to provide reliable estimation of layer thickness.[36] The theoretical height of a molecule of DPPC was determined by ChemDraw and the result obtained, 2.14 nm, was in accordance with that obtained from the scratch. In this regard, a scheme of the DPPC molecule is depicted in the figure 3 of the Annex.

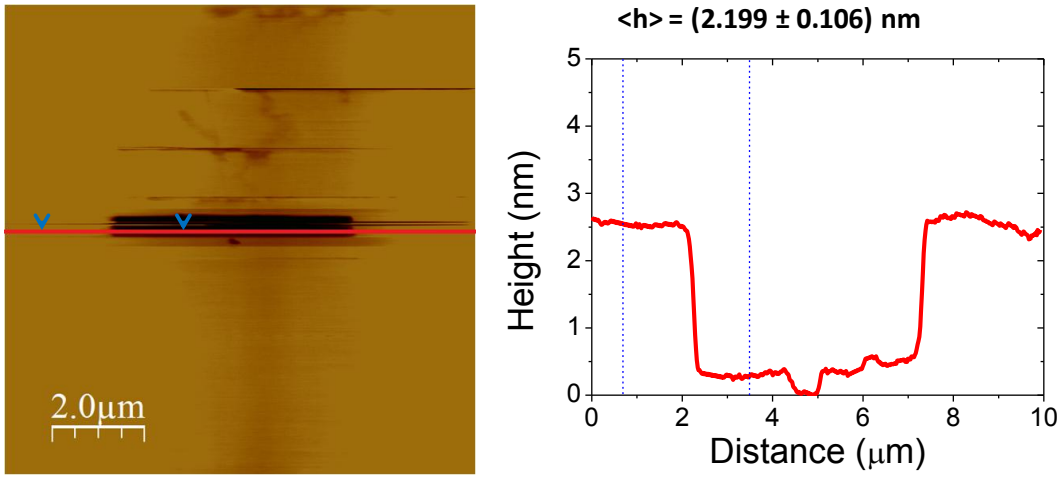

Figure 11. 10 x 10 µm^2 AFM image (left) recorded after scratching a x_{DPPC} = 0.5 monolayer with the AFM tip and the height vs. distance graph (right) used to determine the thickness of the film.

4.5 Contact Angle measurements

In order to analyze the quality of the monolayer transferred by LB and to confirm if the monolayer is transferred onto the solid substrate in a properly way some measurements of contact angle were carried out.

As mentioned above bare mica is highly hydrophilic with water exhibiting contact angle values smaller than ten degrees. In contrast, when the monolayers of DPPC/cholesterol are deposited onto the mica substrate, the surface properties of mica change dramatically,[37] showing contact angles around 86º (Figure 12).

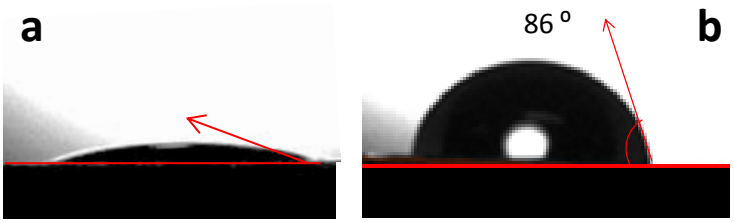

Figure 12. (a) Image of a drop of Milli-Q water onto hydrophilic surface; (b) image of a drop of Milli-Q water onto a mica substrate covered by a monolayer of $x_{DPPC} = 0.5$

In contrast, if a second layer is transferred and a bilayer is present on the surface of mica, then the surface is noticeably hydrophilic, with a contact angle smaller than 10º. Table III gathers the contact angle values of water onto bare mica, a monolayer and a bilayer as well as a proposed orientation of the mono and bilayer films on the mica surface.

Table III. Contact angle for bare mica, a $x_{DPPC} = 0.5$ monolayer and bilayer.

Material	Type	Contact angle(θ)	Cartoon
Mica substrate	Hydrophilic	$< 10^0$	
Monolayer $x_{DPPC} = 0.5$	Hydrophobic	86^0	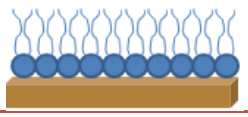
Bilayer $x_{DPPC} = 0.5$	Hydrophilic	$< 10^0$	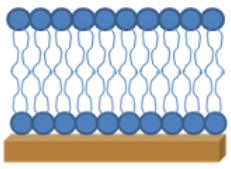

4.6 Stability of the monolayers in liquid media, Breakthrough Force studies

By imaging lipid layers in liquid media, not only their topographical features and molecular structure but also their mechanical properties have been unraveled.[38,39,40] In this context, the effect of immersing these monolayers in aqueous solution has been studied by means of AFM. Thus, when the x_{DPPC} = 0.5 monolayer is placed in an aqueous environment, the molecules in the monolayer, initially located on the mica substrate, spontaneously self-assemble to form a bilayer, and, consequently, different intermediate organization levels are observed depending on the immersion time in the aqueous media.

In order to analyze the influence of the media, a monolayer of x_{DPPC} = 0.5 was placed in the liquid cell of the AFM for different immersion times, t_i. The experiments were performed either in Milli-Q water or in 50 µL of 10 mM HEPES buffer (pH 7.4), which exhibits a low ionic strength to mimic the physiological conditions in a cell membrane. The recorded sequence of images for the x_{DPPC} = 0.5 monolayer in contact with HEPES buffer is shown in Figure 13, where some noticeable structural changes, clearly detectable in the cross section profiles of the sample, can be observed. The different height of the domains in the AFM images are in good agreement with a transition from an initial monolayer (Figure 13.a), to the formation of a partial bilayer (Figure 13.b) and finally a complete bilayer (Figure 13.c). In fact, the cross-section profile shown in Figure 13.c corresponds to the thickness of a bilayer completely formed leaving free zones of bare mica.

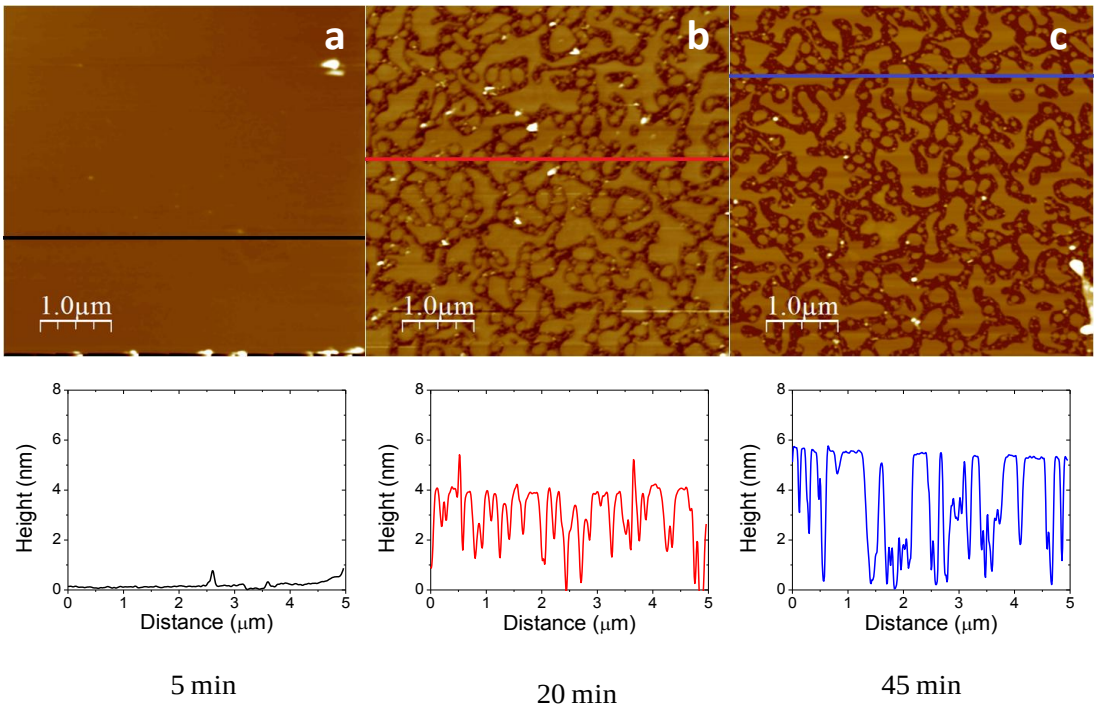

Figure 13. AFM 5.0 x 5.0 µm^2 images and representative cross section analysis of a x_{DPPC} = 0.5 monolayer immersed in 50µL of 10 mM HEPES (pH 7.4) showing the transition from monolayer to bilayer upon the following immersion times: (a) t_i = 5 min.; (b) t_i = 20 min; and (c) t_i = 45 min.

Accordingly, the height histograms (which indicate the height versus the amount of times that this value of height is repeated, it is acquired by a function of NanoScope Analysis software) obtained for the x_{DPPC} = 0.5 monolayer on mica at different immersion times are shown in Figure 14 to account for the height difference occurred during the spontaneous transition from monolayer to bilayer. It can be observed that in the very beginning of the experiment, black histogram, there are no noticeable changes in the morphology and thickness, when compared to that observed for in-air AFM images, i.e. x_{DPPC} = 0.5 monolayer in Figure 10. Therefore, the height value distribution for short immersion times only reflects the surface roughness of the highly smooth x_{DPPC} = 0.5 monolayer. However, as the immersion time increases, a progressive process of formation of an upper layer over the underlying monolayer can be observed, red histogram, accompanied by a progressive appearance of bare mica surface.

Finally, after long exposure times to the solution the height of a complete bilayer was detected. The height histogram corresponding to t_i = 45 min. (Figure 14, blue) shows two maximums at 3.8 and 4.5 nm associated with an incomplete lying-down molecule arrangement above the underlying monolayer (corresponding to the 28.1% of

the projected area, as deduced from the bearing analysis depicted in Figure 4 of the Annex), and an arising vertical assembly of the upper layer (a 37.02% of the projected area, Figure 4 in the Annex section), respectively. Both arrangements would coexist as a progressive enriching in the second maximum upon immersion time is detected. Table IV summarizes these observations.

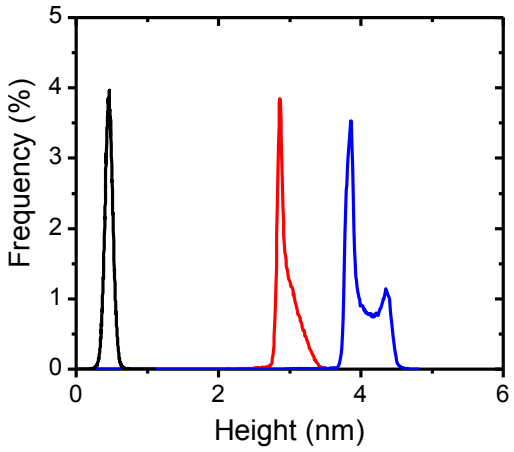

Figure 14. Histograms showing the distribution of height values within the sample at the beginning of the experiment, 5 min., black line, at 20 min., red, and 45 min later, blue, corresponding to the AFM images shown in Figure 13.

Table IV. Mean height of a x_{DPPC} = 0.5 monolayer on mica at growing immersion times in a HEPES buffer solution.

Time (min)	Height average (nm)
5	0.45
20	2.11
45	4.35

To gain more information about the reorganization process of the monolayer in the presence/absence of a liquid medium, representative adhesion images and their corresponding histograms were obtained as illustrated in Figure 15. Each image represents the adhesion effect caused by the interaction between the tip and the sample. In monolayers the tip is expected to interact with the hydrophobic section of the DPPC and cholesterol (see cartoons in Table III). In contrast, in bilayers the tip is expected to interact with the hydrophilic section of the DPPC and cholesterol. Thus, since the tip-sample interaction has a different nature depending on whether there is a monolayer, an

incomplete upper layer or a bilayer, a differential adhesion mapping associated with the topographic image is obtained as can be verified in Figure 15. In the histograms shown in Figure 15 the distribution of the corresponding adhesion values can be observed. Thus, the red histogram, corresponding to both the monolayer and, taking into account the cross section shown in Figure 13b and the height histograms, red, in Figure 14, to an incomplete lying-down phospholipid arrangement above the latter, reveals a Gaussian distribution with a maximum at 122 pN. On the other hand, the blue histogram, corresponding mostly to a bilayer, shows a bimodal distribution with two maximums, at 122 and 178 pN, reflecting the contributions due to the remaining monolayer/ incomplete upper layer zones, green line, and the arising bilayer areas, as the incubation time increases, magenta.[41]

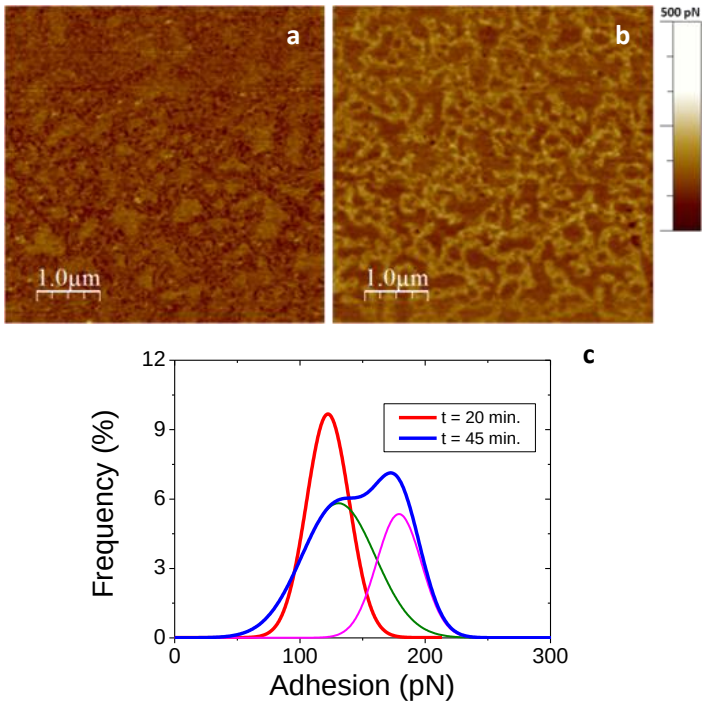

Figure 15. AFM 5.0 x 5.0 µm^2 adhesion images of a x_{DPPC} = 0.5 monolayer *in 50µL of 10 mM HEPES (pH 7.4) solution for the indicated immersion times: (a)* t_i *= 20 min., and (b)*t_i *= 45 min. The adhesion histograms exhibit a Gaussian distribution corresponding mainly to the monolayer, red line, and a bimodal distribution in the case of the bilayer, blue. The latter can be deconvoluted in two different contributions at 122, green line, and 178 pN, magenta line.*

In order to analyze the reversibility of the process (formation of a monolayer after the drying process of the bilayer), an identical study of the above depicted experiments was performed in Milli-Q water, due to the fact that remaining salt crystals caused by the evaporation of the buffer HEPES would not result in clean AFM

topographic images. Figure 16 illustrates the reversibility of the process. Thus, after the re-assembly of the initial monolayer, Figure 16.a, into bilayer domains leaving free mica areas in between, as can be deduced from the height figures extracted from the cross section, Figure 16.b, the initial characteristic topographic features corresponding to the monolayer are restored after the drying process, Figure 16.c.

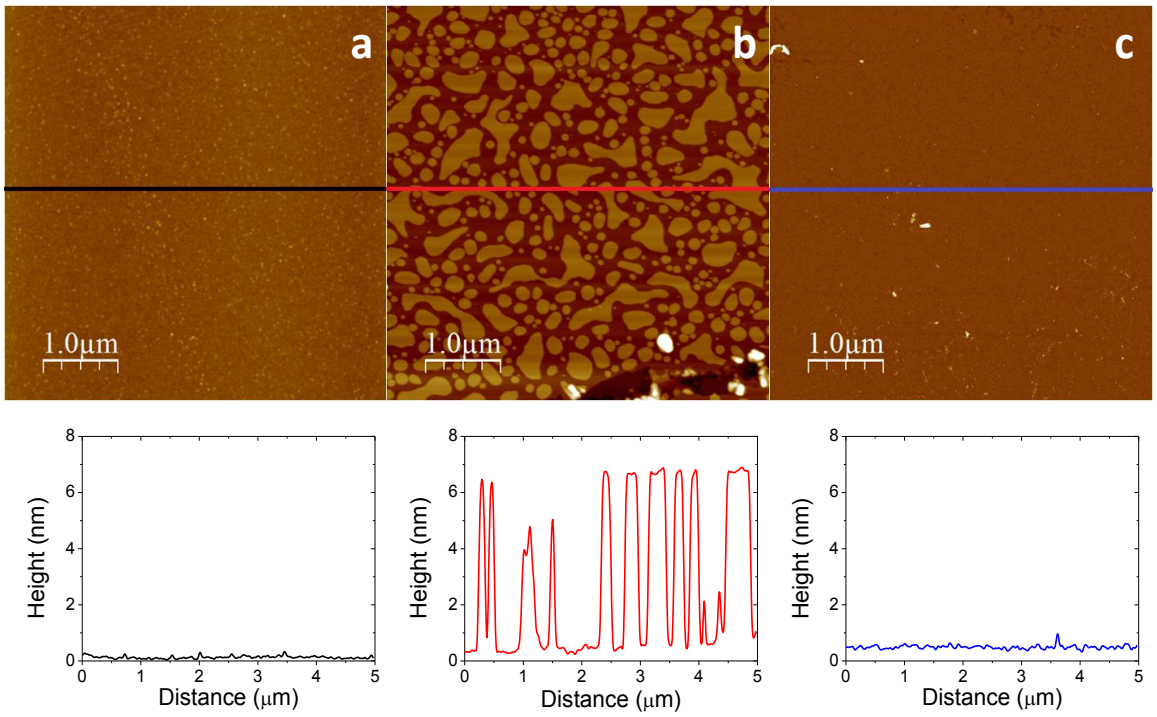

Figure 16. AFM topographic images corresponding to (a) a x_{DPPC} = 0.5 monolayer*; (b) the bilayer formed after 60 minutes; and (c) the monolayer after water was dried. Additionally, the cross-section figures are included.*

The remarkable effect above depicted opens the possibility to study and compare in further detail the nanomechanical properties exhibited by the initial monolayers and the as-formed bilayers in physiological conditions by means of a force-curve study carried out by AFM. In this context, breakthrough force studies have been elsewhere employed to characterize the response of phospholipids membranes under compression.[42,43,44] Thus, in a typical force study FS experiment, a force-curve graph is obtained when an AFM tip is approached to the surface and then a mechanical contact with the lipid layer is produced.[45] Thereafter, this lipid layer is compressed by the AFM tip at growing loading forces and, consequently, its mechanical properties can be quantified. It should be noted that the lipid layers are elastically deformed by the AFM probe until its sharp conical tip ruptures dramatically the lipid layer getting into contact

with the underlying rigid mica substrate. This is translated into a significant jump in the repulsive force-curve slope which is accordingly named as the breakthrough force and resembles unambiguously the onset of the plastic regime.[42]

In this regard, in order to further demonstrate this spontaneous reversible transition from monolayer to bilayer in a liquid environment, a detailed study of the registered force curves versus the piezoelectric displacement was performed on the at different immersion times. These results are summarized in Figure 17.

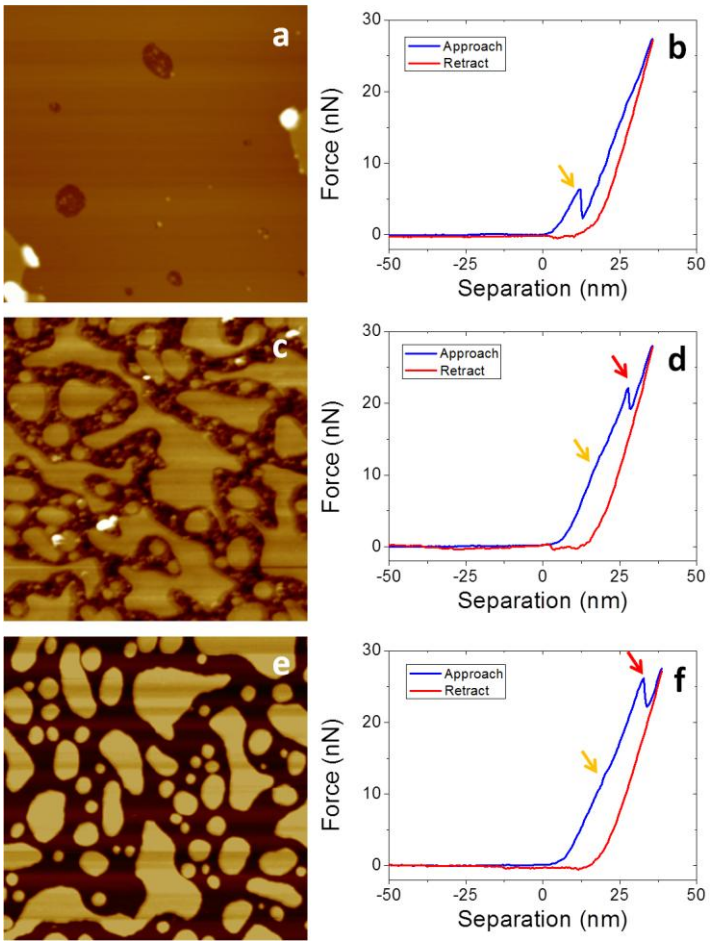

Fig 17. 2.0 x 2.0 µm^{2}AFM images of x_{DPPC} = 0.5 films in 50 µL of 10 mM HEPES (pH 7.4) at different immersion times: (a) t_i = 10 min); (c) t_i = 25 min; and (e) t_i = 50 min. Representative loading force versus separation curves obtained for x_{DPPC} = 0.5 films in 50 µL of 10 mM HEPES (pH 7.4) at different immersion times: (b) t_i = 10 min ; (d) t_i = 25 min; and (f) t_i = 50 min.

For immersion times below 10 min., the jump (yellow arrow) observed in the force curve graph, Figure 17.b, reflects the penetration through the mixed monolayer. On the other hand, for immersion times above 10 min., the resulting force curves, Figure 17.d and f, exhibit a discontinuous jump at higher loading forces (red arrow) and

also a small shoulder at lower forces (yellow arrow) which can be attributed to the rupture of the upper layer and the subsequent underlying monolayer. The breakthrough force values resulted in higher figures as immersion time increases as a consequence of the progressive self-assembly of the phospholipids molecules in a more dense and compact arrangement in the upper layer.

Table V. Mean breakthrough force for a x_{DPPC} = 0.5 monolayer on mica at growing immersion times in a HEPES buffer solution.

Sample	Breakthrough force (nN)
t = 0-10 min.	7.28 ± 1.48
t = 10-30 min.	20.28 ± 1.95
t > 30 min.	25.83 ± 2.77

These results, shown in Table V, are in very good agreement with those previously reported elsewhere by Sanz and co-workers and also Fukuma and co-workers.[43,38,46] Therefore, it can be concluded that for long immersion times (t_i > 30 min.), the x_{DPPC} = 0.5 bilayer domains formed in 10 mM HEPES buffer (pH 7.4) from the x_{DPPC} = 0.5 monolayer, figure 17.e, exhibit nanomechanical properties and stability under compression, figure 17.f, analogue to DPPC/ Cholesterol bilayers obtained by other different methods.[46,42,38, 43]

4.7 Deposition of Magnetic Nanoparticles

Once the lipid monolayer was fabricated and characterized, the next step was immobilizing the magnetic nanoparticles onto the previously fabricated monolayers. In this sense, monodisperse Fe_3O_4 nanoparticles of 8 nm mean diameter used in this work were synthesized according to the methodology developed by Martinez de la Fuente and co-workers.[47] These MNPs are covered with oleic acid and oleyamine. The capping of the MNPs is conveniently selected with the aim to provide a good interaction with the non-polar moiety of the lipid monolayer.

Several methods for depositing nanoparticles onto monolayers have been reported such as SA, drop casting, spin coating and LB among others.[5] In our case, the Self-Assembly (SA) procedure was discarded since incubation in organic solvents could attack or dissolve the monolayer whereas in aqueous media a reorganization into bilayer

domains with free bare mica areas in between is expected.[48] Accordingly LB technique was chosen to this end. The results obtained by LB were noticeable in terms of a good control on the deposition and organization of the assembly of the MNPs onto the monolayer. [10]

Different solutions of these MNPs were prepared in chloroform, water and n-hexane. The results obtained by LB showed that when MNPs were dispersed in n-hexane, a better surface dispersion was observed. However, in water or chloroform, higher levels of nanoparticles aggregation were noticed, these data are not shown in this work. In Figure 18 a Transmission Electron Microscopy (TEM) image of the 8 nm Fe_3O_4 hydrophobic nanoparticles (MNPs) is shown. For further details see the reference. [47]

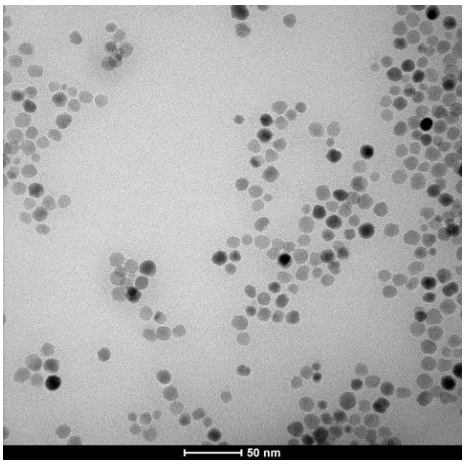

Figure 18 . TEM image of the 8 nm Fe_3O_4 hydrophobic nanoparticles (MNPs).

Figure 19 shows representative AFM images of MNPs deposited onto a x_{DPPC} = 0.5 LB film. MNPs were transferred at surface pressures of 5 and 15 $mN \cdot m^{-1}$. As shown in Figure 19.a, MNPs transferred at 5 $mN \cdot m^{-1}$ exhibit a low surface coverage, although the nanoparticles are well dispersed. In contrast, in Figure 19.b, for NPs transferred at 15 $mN \cdot m^{-1}$, a large surface coverage is achieved accompanied by a regular distribution of the MNPs. A cross-section study to show the average height of the nanoparticles[49] is also shown in Figure 19. The average height of the MNPs is in the 7-8 nm range.

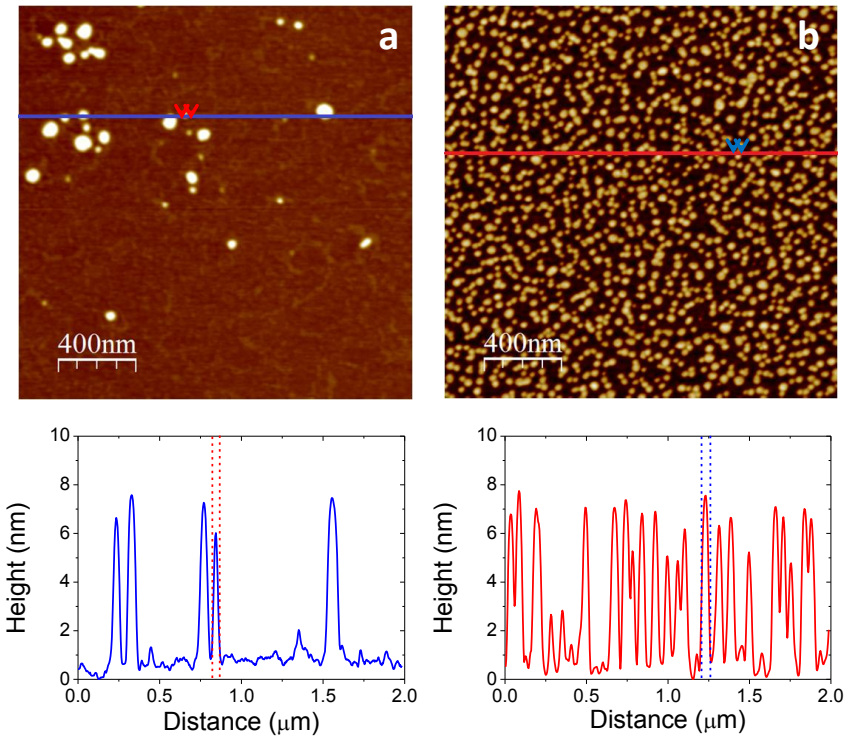

Figure 19. *AFM 2.0 X 2.0 μm^2 topographic images of x_{DPPC} = 0.5 and MNPs transferred at (a) at 5 mN·m^{-1}; (b) at 15 mN·m^{-1} together with their corresponding cross-sections.*

4.8 Hyperthermia studies

All the studies carried out in this project were developed with the aim of studying the effect generated when an alternating magnetic field is applied to the monolayer with the magnetic nanoparticles deposited onto it and to study by AFM how this will affect to the MNPs and to a cell membrane as well.

In order to carry out these experiments one of the main obstacles to solve has to do with being able to come back with the AFM setup to measure exactly the same area within the sample, before and after applying hyperthermia treatment. This is aimed to characterize the local effect of the applied alternating magnetic field on the assembled MNPs and their local environment.

Several attempts were carried out and, finally, a solution for this major impediment was found out. This procedure can be summarized in three different steps:

1. Four 30 x 30 μm^2 squared marks separated from each other by 100 μm were made by Focused Ion Beam (FIB) etching in Si_3N_4 membranes in the clean room at INA. Identical and concentrical marks but, in this case, of 3.0 x 3.0 μm^2 and separated from each other 30 μm were also

addressed. Figure 5.a of annex section shows a photograph of the marked mica with the incorporated squared features described. Both the large outer squares and the small inner ones are clearly visible.

2. A successive evaporation of 5 nm Cr + 75 nm Cu onto the mica surface and through the patterned membrane was carried out. Figure 5.b of annex section exhibits a 3D AFM image of a successfully modified bare mica substrate with the inner marks. Dimensions of the latter (3.0 μm wide and 80 nm high) are depicted in Figure 5.c of the annex section.
3. AFM imaging of the bare mica within the inner marks to confirm that the evaporation process has not affected the topography of the substrate.

Once this patterned mica surfaces are obtained, the whole AFM operational process can be described as follows: firstly, each mark evaporated in the bare mica was verified by AFM measurements to ensure that the internal area was clean. Secondly, x_{DPPC} = 0.5 monolayer was transferred at 35 mN· m^{-1} onto the marked mica and several AFM images at different sizes, always within the inner marks, were carried out to verify the monolayer deposition. In the third step, MNPs were deposited onto the monolayer at 15 mN·m^{-1} and AFM imaging on exactly the same area previously measured was carried out. After that, hyperthermia treatment was applied for 90 minutes. Finally, comparative analyses of the AFM images registered before and after hyperthermia have been made. As can be observed in the Figure 20, noticeable changes took place. A surface diffusion of certain MNPs is detected by AFM imaging when an external alternating magnetic field is applied. For instance, when comparing topographic features present in Figure 20.a and 20.b the disappearance of certain MNPs, red circle, can be detected due to the effect of the applied magnetic field. In contrast, in figure 20.c and d the appearance of a significant amount of MNPs after the hyperthermia experiment.

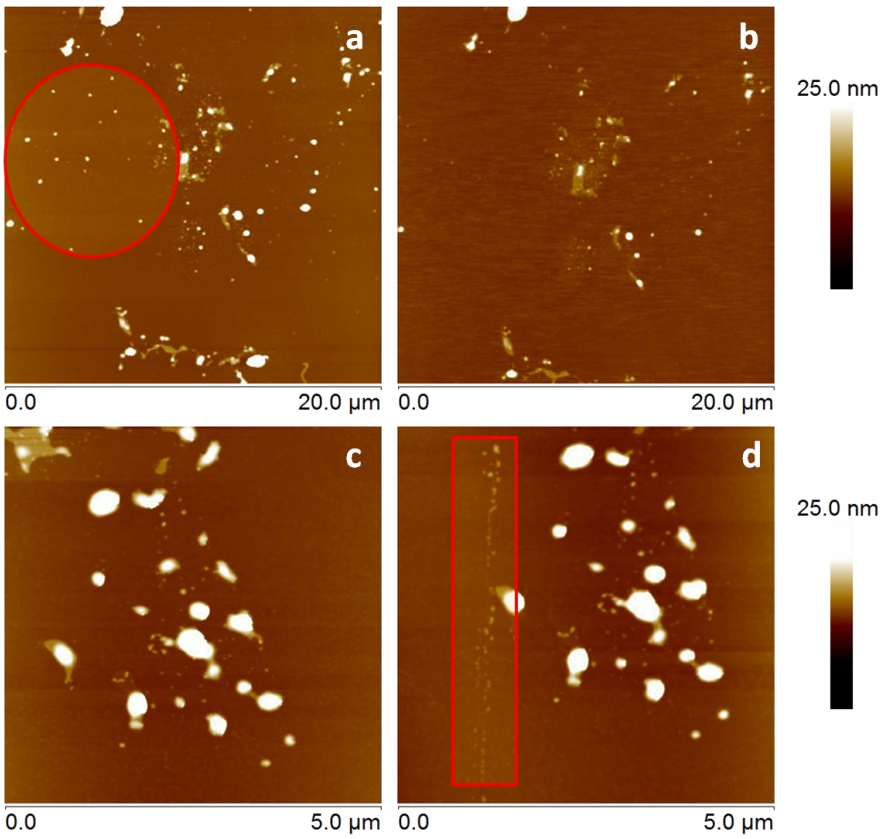

Figure 20. 20.0 x 20.0 µm^2 AFM images (upper panel) and 5.0 x 5.0 µm^2 AFM images (lower panel) of MNPs deposited at 15 mN·m^{-1} on x_{DPPC} = 0.5 monolayer: (a) and (c) before hyperthermia treatment; (b) and (d) after 90 minutes of hyperthermia treatment.

The above described results, although rather promising, are only preliminary experiences aimed at exploring the viability of the whole strategy developed in this work to properly characterize the response exhibited by both the MNPs and the underlying lipid monolayers supported on mica when an external alternating magnetic field is applied.

Chapter 5. Conclusions

The main conclusions obtained from this final master project are summarized in the next lines:

- Mixed monolayers of DPPC lipid and Cholesterol, which are perfectly oriented films and free of holes or three dimensional structures, have been achieved to mimic a cell membrane by means of LB.
- When a lipid monolayer is immersed into an aqueous media, it acquires spontaneously a bilayer-domain structure leaving free mica surface in between. This process has also been demonstrated to be reversible: once the sample is completely dried, the morphological features exhibited by the initial monolayer were restored. Force Spectroscopy studies also corroborated the re-arrangement into a bilayer in terms of a noticeable increase in the breakthrough force of the phospholipid layers.
- A squared Cr-Cu pattern onto the mica substrates was successfully designed and fabricated with the aim to carry out AFM imaging of exactly the same assembled MNPs, before and after the hyperthermia experiences.
- A homogeneous immobilization of the MNPs onto the monolayer surface has been achieved by means of LB, obtaining a well-covered MNP distribution as depicted in AFM images.
- Preliminary hyperthermia studies carried out in this work showed promising results in terms of a significant surface diffusion detected for a noticeable amount of the assembled MNPs as a consequence of applying an alternating magnetic field. These experiences will be the subject of further works on the basis of these hopeful precursory results.

References

1. Tanaka, M.; Sackmann, E., Polymer-supported membranes as models of the cell surface. *Nature* **2005,** *437* (7059), 656-663.
2. Martin, D., *Nanobiotechnology of Biomimetic Membranes*. Springer Science & Business Media: 2007; Vol. 1.
3. Pomorski, T. G.; Nylander, T.; Cárdenas, M., Model cell membranes: Discerning lipid and protein contributions in shaping the cell. *Advances in Colloid and Interface Science* **2014,** *205*, 207-220.
4. Castellana, E. T.; Cremer, P. S., Solid supported lipid bilayers: From biophysical studies to sensor design. *Surface Science Reports* **2006,** *61* (10), 429-444.
5. Roiter, Y.; Ornatska, M.; Rammohan, A. R.; Balakrishnan, J.; Heine, D. R.; Minko, S., Interaction of Nanoparticles with Lipid Membrane. *Nano Letters* **2008,** *8* (3), 941-944.
6. El Kirat, K.; Morandat, S.; Dufrêne, Y. F., Nanoscale analysis of supported lipid bilayers using atomic force microscopy. *Biochimica et Biophysica Acta (BBA) - Biomembranes* **2010,** *1798* (4), 750-765.
7. Szoka Jr, F.; Papahadjopoulos, D., Comparative properties and methods of preparation of lipid vesicles (liposomes). *Annual review of biophysics and bioengineering* **1980,** *9* (1), 467-508.
8. Eeman, M.; Deleu, M., From biological membranes to biomimetic model membranes. *Base* **2010**.
9. Mueller, P.; Rudin, D. O.; Ti Tien, H.; Wescott, W. C., Reconstitution of cell membrane structure in vitro and its transformation into an excitable system. *Nature* **1962,** *194*, 979-980.
10. Miyashita, T., Recent studies on functional ultrathin polymer films prepared by the Langmuir-Blodgett technique. *Progress in Polymer Science* **1993,** *18* (2), 263-294.
11. Maget-Dana, R., The monolayer technique: a potent tool for studying the interfacial properties of antimicrobial and membrane-lytic peptides and their interactions with lipid membranes. *Biochimica et Biophysica Acta (BBA) - Biomembranes* **1999,** *1462* (1–2), 109-140.
12. Levine, Y. K.; Bailey, A. I.; Wilkins, M. H. F., Multilayers of Phospholipid Bimolecular Leaflets. *Nature* **1968,** *220* (5167), 577-578.
13. Kuhn, H.; Möbius, D.; Bücher, H., Spectroscopy of monolayer assemblies. *Physical methods of chemistry* **1972,** *1* (Part 3).
14. Korenbrot, J.; Pramik, M.-J., Formation, structure, and spectrophotometry of air-water interface films containing rhodopsin. *J. Membrain Biol.* **1977,** *37* (1), 235-262.
15. Murthy, S. K., Nanoparticles in modern medicine: State of the art and future challenges. *International Journal of Nanomedicine* **2007,** *2* (2), 129-141.
16. Hu, C.-M. J.; Fang, R. H.; Wang, K.-C.; Luk, B. T.; Thamphiwatana, S.; Dehaini, D.; Nguyen, P.; Angsantikul, P.; Wen, C. H.; Kroll, A. V.; Carpenter, C.; Ramesh, M.; Qu, V.; Patel, S. H.; Zhu, J.; Shi, W.; Hofman, F. M.; Chen, T. C.; Gao, W.; Zhang, K.; Chien, S.; Zhang, L., Nanoparticle biointerfacing by platelet membrane cloaking. *Nature* **2015,** *526* (7571), 118-121.
17. Bañobre-López, M.; Teijeiro, A.; Rivas, J., Magnetic nanoparticle-based hyperthermia for cancer treatment. *Reports of Practical Oncology & Radiotherapy* **2013,** *18* (6), 397-400.
18. Silvio, D.; Rudolf, H., Magnetic particle hyperthermia—a promising tumour therapy? *Nanotechnology* **2014,** *25* (45), 452001.
19. Frey, N. A.; Peng, S.; Cheng, K.; Sun, S., Magnetic nanoparticles: synthesis, functionalization, and applications in bioimaging and magnetic energy storage. *Chemical Society Reviews* **2009,** *38* (9), 2532-2542.

20. Brockman, H., Lipid monolayers: why use half a membrane to characterize protein-membrane interactions? *Current Opinion in Structural Biology* **1999,** *9* (4), 438-443.
21. Zasadzinski, J. A.; Helm, C. A.; Longo, M. L.; Weisenhorn, A. L.; Gould, S. A.; Hansma, P. K., Atomic force microscopy of hydrated phosphatidylethanolamine bilayers. *Biophysical Journal* **1991,** *59* (3), 755-760.
22. Egawa, H.; Furusawa, K., Liposome Adhesion on Mica Surface Studied by Atomic Force Microscopy. *Langmuir* **1999,** *15* (5), 1660-1666.
23. Kim, K.; Kim, C.; Byun, Y., Preparation of a Dipalmitoylphosphatidylcholine/Cholesterol Langmuir−Blodgett Monolayer That Suppresses Protein Adsorption. *Langmuir* **2001,** *17* (16), 5066-5070.
24. Vist, M. R.; Davis, J. H., Phase equilibria of cholesterol/dipalmitoylphosphatidylcholine mixtures: deuterium nuclear magnetic resonance and differential scanning calorimetry. *Biochemistry* **1990,** *29* (2), 451-464.
25. Ginzburg, V. V.; Balijepalli, S., Modeling the Thermodynamics of the Interaction of Nanoparticles with Cell Membranes. *Nano Letters* **2007,** *7* (12), 3716-3722.
26. Verma, A.; Stellacci, F., Effect of Surface Properties on Nanoparticle–Cell Interactions. *Small* **2010,** *6* (1), 12-21.
27. Berquand, A.; Mingeot-Leclercq, M. P.; Dufrêne, Y. F., Real-time imaging of drug–membrane interactions by atomic force microscopy. *Biochimica et Biophysica Acta (BBA) - Biomembranes* **2004,** *1664* (2), 198-205.
28. Petty, M. C., *Langmuir-Blodgett films: an introduction*. Cambridge University Press: 1996.
29. Jurak, M., Thermodynamic Aspects of Cholesterol Effect on Properties of Phospholipid Monolayers: Langmuir and Langmuir–Blodgett Monolayer Study. *The Journal of Physical Chemistry B* **2013,** *117* (13), 3496-3502.
30. Wydro, P.; Knapczyk, S.; Łapczyńska, M., Variations in the Condensing Effect of Cholesterol on Saturated versus Unsaturated Phosphatidylcholines at Low and High Sterol Concentration. *Langmuir* **2011,** *27* (9), 5433-5444.
31. Haro, M.; Giner, B.; Lafuente, C.; López, M. C.; Royo, F. M.; Cea, P., Proton Sponge and Fatty Acid Interactions at the Air−Water Interface. Thermodynamic, Spectroscopic, and Microscopic Study. *Langmuir* **2005,** *21* (7), 2796-2803.
32. Marsh, D., Lateral pressure in membranes. *Biochimica et Biophysica Acta (BBA) - Reviews on Biomembranes* **1996,** *1286* (3), 183-223.
33. Johnston, L. J., Nanoscale Imaging of Domains in Supported Lipid Membranes. *Langmuir* **2007,** *23* (11), 5886-5895.
34. Mingeot-Leclercq, M.-P.; Deleu, M.; Brasseur, R.; Dufrene, Y. F., Atomic force microscopy of supported lipid bilayers. *Nat. Protocols* **2008,** *3* (10), 1654-1659.
35. Hane, F.; Moores, B.; Amrein, M.; Leonenko, Z., Effect of SP-C on surface potential distribution in pulmonary surfactant: Atomic force microscopy and Kelvin probe force microscopy study. *Ultramicroscopy* **2009,** *109* (8), 968-973.
36. Anariba, F.; DuVall, S. H.; McCreery, R. L., Mono- and Multilayer Formation by Diazonium Reduction on Carbon Surfaces Monitored with Atomic Force Microscopy "Scratching". *Analytical Chemistry* **2003,** *75* (15), 3837-3844.
37. Kwok, D. Y.; Neumann, A. W., Contact angle measurement and contact angle interpretation. *Advances in Colloid and Interface Science* **1999,** *81* (3), 167-249.
38. Redondo-Morata, L.; Giannotti, M. I.; Sanz, F., Influence of Cholesterol on the Phase Transition of Lipid Bilayers: A Temperature-Controlled Force Spectroscopy Study. *Langmuir* **2012,** *28* (35), 12851-12860.
39. Jurak, M., Changes in stability of the DPPC monolayer during its contact with the liquid phase. *Chemistry and Physics of Lipids* **2012,** *165* (3), 302-310.

40. Pinnow, M., Lipid and biopolymer monolayers at liquid interfaces. Von K. S. BIRDI. ISBN 0-306-42870-9. New York/Londen: Plenum Press 1989. X, 325 S., geb., US $ 59.50 (outside USA and Canada US $ 71.40). *Acta Polymerica* **1990,** *41* (5), 314-314.
41. Tanem, B. S.; Lunder, O.; Borg, A.; Mårdalen, J., AFM adhesion force measurements on conversion-coated EN AW-6082-T6 aluminium. *International Journal of Adhesion and Adhesives* **2009,** *29* (5), 471-477.
42. Garcia-Manyes, S.; Oncins, G.; Sanz, F., Effect of Ion-Binding and Chemical Phospholipid Structure on the Nanomechanics of Lipid Bilayers Studied by Force Spectroscopy. *Biophysical Journal* **2005,** *89* (3), 1812-1826.
43. Garcia-Manyes, S.; Redondo-Morata, L.; Oncins, G.; Sanz, F., Nanomechanics of Lipid Bilayers: Heads or Tails? *Journal of the American Chemical Society* **2010,** *132* (37), 12874-12886.
44. Dols-Perez, A.; Fumagalli, L.; Simonsen, A. C.; Gomila, G., Ultrathin Spin-Coated Dioleoylphosphatidylcholine Lipid Layers in Dry Conditions: A Combined Atomic Force Microscopy and Nanomechanical Study. *Langmuir* **2011,** *27* (21), 13165-13172.
45. Dufrene, Y. F.; Martinez-Martin, D.; Medalsy, I.; Alsteens, D.; Muller, D. J., Multiparametric imaging of biological systems by force-distance curve-based AFM. *Nat Meth* **2013,** *10* (9), 847-854.
46. Hitoshi, A.; Takeshi, F., The molecular-scale arrangement and mechanical strength of phospholipid/cholesterol mixed bilayers investigated by frequency modulation atomic force microscopy in liquid. *Nanotechnology* **2009,** *20* (26), 264008.
47. Moros, M.; Pelaz, B.; Lopez-Larrubia, P.; Garcia-Martin, M. L.; Grazu, V.; de la Fuente, J. M., Engineering biofunctional magnetic nanoparticles for biotechnological applications. *Nanoscale* **2010,** *2* (9), 1746-1755.
48. Hod, M.; Dobbrow, C.; Vaidyanathan, M.; Guin, D.; Belkoura, L.; Strey, R.; Gottlieb, M.; Schmidt, A. M., Controlling the self-assembly of magnetic nanoparticles by competing dipolar and isotropic particle interactions. *Journal of Colloid and Interface Science* **2014,** *436*, 83-89.
49. Milhiet, P.-E.; Gubellini, F.; Berquand, A.; Dosset, P.; Rigaud, J.-L.; Le Grimellec, C.; Lévy, D., High-Resolution AFM of Membrane Proteins Directly Incorporated at High Density in Planar Lipid Bilayer. *Biophysical Journal 91* (9), 3268-3275.